Int. J. Heat Mass Transfer. Vol. 29, No. 5, pp. 797–807, 1986
Printed in Great Britain

0017–9310/86 $3.00 + 0.00
Pergamon Journals Ltd.

Laminar forced convection in circular and flat ducts with wall axial conduction and external convection

N. E. WIJEYSUNDERA
Department of Mechanical and Production Engineering, National University of Singapore, Kent Ridge, Singapore 0511

(*Received* 11 *July* 1985 *and in final form* 10 *December* 1985)

Abstract—An analytical solution is obtained for laminar forced convection in circular and flat ducts with the presence of axial duct wall conduction and external convection at the outer surface of the duct wall. The eigenvalues for the problem are determined using the solution for the constant temperature boundary condition. The heat transfer results depend on four nondimensional numbers. The wall and fluid temperatures depend strongly on the wall conductance parameter while the heat flux enhancement due to wall conduction is large at short distances from the duct inlet.

INTRODUCTION

LAMINAR forced convection in round pipes and flat ducts is an important heat transfer situation encountered in many engineering applications. This problem has been solved for various boundary conditions including the constant wall temperature, the constant wall heat flux and the external convective heat transfer. The literature on the solution for these boundary conditions is reviewed by Shah and London [1]. As Shah [2] points out, the laminar convection problem with simultaneous duct wall axial conduction has received less attention. The effect of wall axial conduction on laminar flow heat transfer was studied by Davis and Gill [3] and Mori *et al.* [4, 5]. Mori *et al.* considered round and flat ducts with the constant wall temperature and constant wall flux boundary conditions. Faghri and Sparrow [6] have extended this study to include axial conduction in the fluid and the duct wall.

The present paper addresses an extension of this problem to include external convection from the conducting duct wall. This situation has applications in the design of natural convection radiators, cross-flow heat exchangers and some solar energy collectors. In these situations, the fluid in the duct is in laminar flow with a heat loss or gain by external convection, at the outer surface of the wall where the external heat transfer coefficient is uniform. An analytical method is developed for the solution of this conjugate heat transfer problem using the Duhamel's superposition technique. A simple procedure is obtained for the determination of the eigenvalues of the solution.

ANALYSIS

In this section an analytical model is developed for the conjugate heat transfer problem. The ducts considered in the study are shown in Figs. 1(a) and (b). The detailed analysis is given for the round pipe and the corresponding results for the flat duct are easily deduced. The conjugate heat transfer problem consisting of the flowing fluid and the tube wall is governed by the respective energy equations. In the present study we are concerned with a thin-walled tube with convective heat transfer at the outer surface. The heat transfer coefficient and the temperature of the external fluid is assumed to be uniform. In order to make the analysis general we also introduce internal heat generation Q in the wall. Since the wall is assumed thin, this could also account for an incident external radient energy source. Applying the energy equation to the tube wall element, the local convective heat flux from the inner surface of the tube to the flowing fluid is obtained as

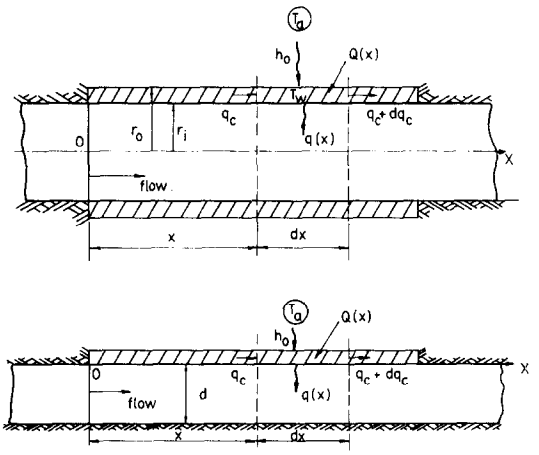

FIG. 1. Schematic diagrams of ducts.

$$q(x) = \left(\frac{r_o h_o}{r_i}\right)(T_a - T_w) + \frac{(r_o^2 - r_i^2)}{2r_i} k_w \left(\frac{d^2 T_w}{dx^2}\right) + \left(\frac{r_o}{r_i}\right) Q(x). \quad (1)$$

NOMENCLATURE

B external Biot number, $h_o r_o/k$
C_p specific heat capacity of the fluid
C_i coefficient in the temperature distribution
C_n coefficient in the constant temperature solution
d width of flat duct
G_n coefficient in the constant temperature solution
h_o external heat transfer coefficient
$H(s)$ function in the solution
k thermal conductivity of the internal fluid
k_w thermal conductivity of the duct wall
L length of the duct
L^+ dimensionless length of the duct, $L/r \cdot Pe$
$\dot{m}$ mass flow rate of fluid
Nu Nusselt number for internal flow, $(h \times 2r_i/k)$
Pe Péclet number of fluid, $u_m(2r_i)/\bar{\alpha}$
$Q(x)$ wall energy source
q_o wall heat flux without wall axial conduction
q_Φ wall heat flux with wall conduction
q heat flux at inner tube wall
q^+ dimensionless heat flux, qr_i/k
r_o outer radius of tube
r_i inner radius of tube
r radial coordinate
r^+ dimensionless radial coordinate, r/r_i
R_n coefficient in solution
s Laplace transform variable
T_o effective external temperature
$T_w(z)$ wall temperature distribution
T_a external fluid temperature
T_e fluid temperature at duct inlet
$T_{fb}(x)$ bulk mean fluid temperature
t_o effective temperature above inlet fluid, $(T_o - T_e)$
t_w wall temperature above inlet fluid, $(T_w - T_e)$
$t_w(0)$ wall temperature at $z = 0$
$t(r^+, z)$ dimensionless fluid temperature
t_{fb} bulk fluid temperature above inlet fluid, $(T_{fb} - T_e)$
$\bar{t}_o$ Laplace transform of t_o
$\bar{t}_w$ Laplace transform of t_w
u_m mean fluid axial speed
$u(r)$ fluid velocity distribution
x axial coordinate
x^+ dimensionless axial coordinate, (x/r_i)
z dimensionless axial coordinate, $x/(r_i Pe)$.

Greek symbols
α_i roots of the equation, $H(s) = 0$
α_p positive root of equation, $H(s) = 0$
$\bar{\alpha}$ thermal diffusivity of fluid
β wall conductance parameter
Φ dimensionless parameter, β/Pe^2
θ function in solution
μ dimensionless parameter, Φ/B
λ_n eigenvalues of solution
ρ density of fluid.

Equation (1) can be written in terms of an effective external fluid temperature $T_o(x)$, in the form

$$q(x) = \left(\frac{r_o h_o}{r_i}\right)(T_o - T_w) + \frac{(r_o^2 - r_i^2)}{2r_i} k_w \left(\frac{d^2 T_w}{dx^2}\right) \quad (1^*)$$

where

$$T_0(x) = \frac{Q(x)}{h_o} + T_a.$$

The boundary conditions for the wall are

$$\frac{dT_w}{dx} = 0, \quad \text{for} \quad x \leqslant 0 \quad \text{and} \quad x \geqslant L.$$

In the absence of a generation source Q, the effective temperature is equal to the external fluid temperature T_a. The energy equation for the fluid is written for hydrodynamically fully developed laminar flow in the absence of fluid axial conduction. For a round pipe this takes the form

$$\rho u C_p \frac{\partial T}{\partial x} = \frac{k}{r} \frac{\partial}{\partial r}\left[r \frac{\partial T}{\partial r}\right] \quad (2)$$

where

$$u(r) = 2u_m \left[1 - \left(\frac{r}{r_i}\right)^2\right].$$

The boundary condition at $r = 0$ is

$$\frac{\partial T}{\partial r}(0, x) = 0, \quad x > 0. \quad (2a)$$

The boundary condition at $x = 0$ is

$$T(r, 0) = T_e. \quad (2b)$$

Equations (1*) and (2) are now expressed in dimensionless form. For this purpose we use the terms similar to those adopted by Faghri and Sparrow [6].

The energy equation for the wall takes the nondimensional form

$$q^+ = \left(\frac{qr_i}{k}\right) = (t_o - t_w)B + \left(\frac{d^2 t_w}{dz^2}\right)\Phi \quad (3)$$

where the external Biot number, $B = (h_o r_o/k)$ and the parameter Φ is given by

$$\Phi = \frac{\beta}{Pe^2}$$

and

$$\beta = \frac{(r_o^2 - r_i^2)}{2r_i^2}\left(\frac{k_w}{k}\right)$$

is the wall conductance parameter.

The Biot number is usually defined as $(h_o r_o/k_w)$ for most conduction–convection situations. In the present instance, however, the thermal resistance of the wall in the radial direction is assumed to be small. The nondimensional number, B, is more a measure of the ratio of the internal fluid resistance to the external convective resistance. This nondimensional number has been used previously in the solution of the Graetz problem with boundary conditions of the third kind [8, 9]. The wall conductance parameter, β, is a measure of the ratio of the axial wall conductance to the conductance of the fluid. The nondimensional number, Φ, is directly proportionally to β, for a constant value of the Péclet number.

The boundary conditions are:

$$\frac{dt_w}{dz} = 0, \quad \text{at} \quad z \leqslant 0 \quad \text{and} \quad z \geqslant L^+$$

Following the work of some of the previous investigators on related conjugate problems, the nondimensional axial coordinate could be taken as, $x^+ = x/r_i$ instead of the more common nondimensional coordinate, $z = x/(r_i Pe)$. This would make the comparison of results with other work easy. However, the presentation of results is considerably compressed by using the parameter z. Hence we develop the analysis using the parameter z as the axial distance variable.

The nondimensional form of the set of equations [2], with constant wall temperature boundary condition $T(r_i, x) = T_o$, has been solved, and the solution is given by Kays [7] in the nondimensional form

$$\theta(r^+, z) = \sum_{n=0}^{\infty} C_n R_n(r^+) \exp(-\lambda_n^2 z). \qquad (2^*)$$

The eigenvalues λ_n and the coefficients G_n for this system are tabulated in ref. [7].

The foregoing expression (2*) is now used to obtain the solution for the set of equations (2) and (3), using the Duhamel superposition technique. This gives the equation

$$-B(t_o - t_w) - \Phi\left(\frac{d^2 t_w}{dz^2}\right) = -q^+$$

$$= \int_0^z t(1, \eta)\left(\frac{d\theta'}{dz}\right)(1, z-\eta)\, d\eta + \theta'(1, 0)\cdot t(1, z) \qquad (4)$$

where $t_w(z) = t(1, z)$.

In order to solve the integro-differential equation (4), the axial distance variable z is Laplace transformed and the convolution theorem is applied to the first term on the RHS. The wall end boundary conditions are applied to second term on LHS in its transformation.

This leads to the equation

$$-B[\bar{t}_o - \bar{t}_w] + \Phi s t_w(0) - \Phi s^2 \bar{t}_w = \theta'(1, 0)\bar{t}_w + \bar{t}_w \bar{\theta} \qquad (5)$$

where

$$\bar{\theta} = \sum_{n=0}^{\infty} \frac{2G_n \lambda_n^2}{(s + \lambda_n^2)}$$

is the Laplace transform of $(d\theta'/dz)$ and

$$\theta'(1, 0) = -2\sum_{n=0}^{\infty} G_n, \text{ from ref. [7].}$$

On substitution equation (5) simplifies to the form

$$\bar{t}_w = \frac{[\bar{t}_o - \mu s t_w(0)]}{\left[(1 - \mu s^2) + \left(\frac{2s}{B}\right)\sum_{n=0}^{\infty} \frac{G_n}{(s + \lambda_n^2)}\right]} \qquad (6)$$

where $\mu = \Phi/B$.

In principle, equation (6) can be used to determine the wall temperature distribution and all the other heat transfer parameters, for any form of the given equivalent external temperature distribution $t_o(z)$. The computational problem reduces to one of determining the zeros of the expression

$$H(s) = (1 - \mu s^2) + \left(\frac{2s}{B}\right)\sum_{n=0}^{\infty} \frac{G_n}{(s + \lambda_n^2)} \qquad (7)$$

and then obtaining the inverse transform of (6).

An accurate iterative method was used to obtain the zeros of $H(s)$ in the present work. This will be described later in the paper. In general, $H(s) = 0$, has only one positive root and all the other roots are negative. If the roots of $H(s) = 0$ are denoted by α_i, then the wall temperature distribution is obtained by inverting expression (6), and for a uniform external temperature distribution t_o, this has the form

$$t_w(z) = t_o + \sum_{i=1}^{\infty} C_i\left[\frac{t_o}{\alpha_i} - \mu t_w(0)\cdot\alpha_i\right] e^{\alpha_i z} \qquad (8)$$

where the coefficient C_i is given by

$$C_i = \left[\frac{2}{B}\sum_{n=0}^{\infty} \frac{G_n \lambda_n^2}{(\alpha_i + \lambda_n^2)^2} - 2\mu\alpha_i\right]^{-1}. \qquad (9)$$

In the temperature distribution given by (8), the wall temperature at $z = 0$, $t_w(0)$ is as yet unknown. This is to be determined using the wall end boundary conditions. Here two situations can be distinguished.

For the first case of a very long duct, the contribution from the positive root α_p must be zero for otherwise the term $e^{\alpha_p z} \to \infty$ as $z \to \infty$.

Therefore, from (8) we obtain the condition

$$\mu t_w(0) = \frac{t_o}{\alpha_p^2}, \quad \text{for a 'long' duct.}$$

For the second case, consider a duct of nondimensional length L^+. The heat flow along the duct wall at $z = L^+$ is zero from the boundary condition assumed. Therefore,

$$\left.\frac{dt_w}{dz}\right|_{z = L^+} = 0.$$

Using equation (8) we have,

$$\mu t_w(0) = \frac{t_o \sum_{i=1}^{\infty} C_i \exp(\alpha_i L^+)}{\sum_{i=1}^{\infty} C_i \alpha_i^2 \exp(\alpha_i L^+)}, \quad \text{for a 'short' duct.}$$

The wall temperature distribution is completely known now and it can be used to obtain closed form expressions for all the other important heat transfer parameters like the bulk mean fluid temperature distribution, the wall heat flux distribution and the local Nusselt number variation. These are summarised in the following section.

Bulk mean fluid temperature

Applying the energy equation to a control volume from $x = 0$ to x we obtain the following

$$2\pi r_o \int_0^x q(x')\,dx' + \dot{m}C_p T_e = \dot{m}C_p T_{fb} + \pi(r_o^2 - r_i^2)k_w\left(\frac{dT_w}{dx}\right) + 2\pi r_o h_o \int_0^x (T_w - T_a)\,dx'. \quad (10)$$

Substitution of the nondimensional variables gives the bulk mean fluid temperature as

$$\frac{t_{fb}}{4B} = \int_0^z [t_o - t_w]\,dz' + \mu\left(\frac{dt_w}{dz}\right). \quad (11)$$

Local heat flux and Nusselt number

Applying the energy equation to a wall element at x we have

$$2\pi r_i q = \dot{m}C_p \frac{dT_{fb}}{dx}. \quad (12)$$

This gives the nondimensional form for the wall heat flux

$$q^+ = \frac{qr_i}{t_o k_f} = \frac{1}{4t_o}\left(\frac{dt_{fb}}{dz}\right). \quad (13)$$

The local Nusselt number is given by

$$Nu = \frac{h_i 2r_i}{k} = \frac{2r_i}{k}\left[\frac{q}{T_w - T_{fb}}\right]. \quad (14)$$

The nondimensional form is

$$Nu = \frac{2q^+ t_o}{(t_w - t_{fb})}. \quad (15)$$

Direct substitution of the expressions given by equations (8) and (9) for the wall temperature, in the equations (11), (13) and (15) gives the various heat transfer parameters.

Computational method

The computational problem associated with the present analytical method reduces essentially to one of finding the roots of the equation, $H(s) = 0$, where $H(s)$ is given by equation (7). The form of the functions involved in $H(s)$, lends itself to an iterative solution which is both fast and accurate. Also there is no difficulty in obtaining the very large roots. Figure 2 shows a sketch of the various functions involved in $H(s)$. It is seen that $(\mu s^2 - 1)$ is parabolic with zero values at $\pm 1/\sqrt{\mu}$ and a turning point at $(0, -1)$. The functional form $(2s/B)\sum_0^\infty G_n/(s + \lambda_n^2)$, has branches lying between a series of asymptotes at the various 'λ_n' values. For large positive values of s, the curve reaches the value $(2/B)\sum_{n=0}^{\infty} G_n$. The intersection of the two functions corresponds to the roots of $H(s) = 0$. It is clear that there is one positive root in range, $1/\sqrt{\mu} < \alpha_p < \infty$. The negative roots lie between the various λ_n values and the larger roots get progressively closer to the corresponding λ_n values. With a reasonable initial value for each root, an iterative procedure converges rapidly on the exact root. This can be achieved with any desired degree of accuracy. In the present computation over 50 roots were used to obtain consistent converged results for the Nusselt number.

The predictions of the present method in the absence of wall conduction, i.e. with $\mu = 0$, were compared with 12 eigenvalues and coefficients given recently by Özişik and Sadeghipour [9], over a range of Biot numbers from 0.10 to 100, for a round tube. The agreement was very good with the maximum deviation less than 0.02%. Next the present results were compared with those of Faghri and Sparrow [8], for local Nusselt number variation in the absence of wall axial con-

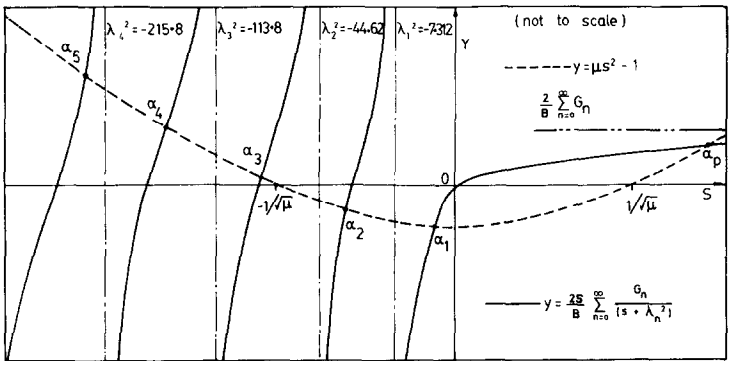

FIG. 2. Roots of $H(s) = 0$.

duction. Over the range of z, from 0.0004 to 1.0, and at Biot numbers of 0.8, 2.1 and 11.2, the differences between the results if any are too small to be resolved using the graphs A′, B′ and E′ in Fig. 1 of ref. [8]. The heat transfer results for the solution of the conjugate problem using the foregoing analysis, are presented in the next section.

RESULTS AND DISCUSSION

It is seen that in view of the many parameters involved in the analysis, a completely general data presentation is difficult. Each heat transfer parameter like the bulk mean fluid temperature and the local Nusselt number depends on three independent dimensionless parameters z, B and Φ, for the case of a 'long' duct and the nondimensional length L^+ becomes an additional parameter for the case of a short duct. The Péclet number, Pe, does not occur as an independent parameter. We take advantage of this fact to compress the presentation of results. Since the Péclet number occurs in Φ and z, it can be treated as a scaling factor in the various curves.

The eigenvalues α_i and coefficients C_i for the round tube and the flat duct are given in Tables 1 and 2, at different values of the conductance parameter Φ and the Biot number B. The sign is consistent with the equation for the wall temperature distribution. The main heat transfer results are discussed in the following section considering first the case of a 'long' duct.

The variation of the tube wall temperature with axial distance is shown in Figs. 3 and 4. It is seen that the wall temperature is influenced both by the wall conductance parameter Φ and the Biot number B. When B is small, i.e. when the external thermal resistance is larger, the wall temperature distribution depends strongly on Φ. The distribution gets progressively 'flatter' as Φ is increased. This is to be expected due to the increased conduction heat flow downstream along the tube wall. For low values of Φ, the increase in wall temperature is more gradual due to the reduced 'fin' effect. When B is increased to a large value, i.e. when the external thermal resistance is very low, the influence of the variation of Φ on the wall temperature distribution is much less and the distribution is much flatter as seen from Fig. 4. Figure 3 shows that for $B = 1.0$, the temperature distributions intersect at distance beyond about $z = 0.3$. The wall temperature for larger Φ values now fall below that for smaller Φ. This is due to the balance which occurs between heat flow along pipe wall, the heat flow by external convection and the heat flow into the fluid. The magnitude of these quantities at any section is determined by the changes which occur along the downstream section.

A similar crossing occurs for the bulk mean fluid temperature distributions as evident from Figs. 5 and 6. However, the effect of the conduction parameter Φ, on the bulk mean temperature is less pronounced. At shorter distances, the 'fin effect' resulting from the heat flow along the tube wall helps to increase the fluid temperature more rapidly. However, as the wall temperature falls below the corresponding value for the low Φ value, the bulk fluid temperature follows this decrease some distance upstream of wall temperature crossing point. The effect of the Biot number B on the bulk mean fluid temperature is significant as seen in Fig. 5. At smaller values of B, the rise is very slow due to the poorer heat gain by external convection.

The effect of the wall conductance on the inner convection heat flux is evident from Fig. 7 where heat flux ratio is plotted against axial distance. In the near region of the tube, the heat flux is increased by a factor of two to three for low Biot number of about 1.0 to 0.10. However, at larger Biot number, the high external convection reduces the enhancement of the heat flux resulting from the 'fin' effect along the tube wall. Thus the wall conduction effects are more important in situations where the external thermal resistances is the controlling factor.

The effect of the wall conductance parameter on the local Nusselt number is less pronounced as seen in Fig.

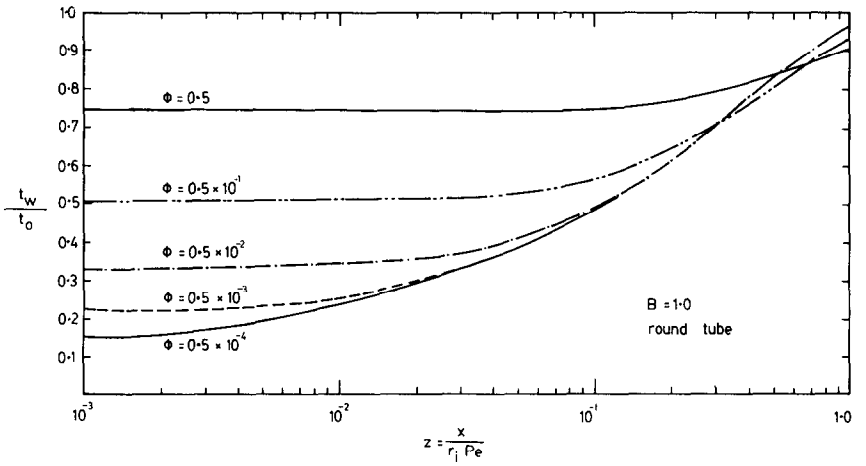

FIG. 3. Axial variation of wall temperature.

Table 1. Eigenvalues and coefficients for round pipe

		$\Phi = 10^{-3}$		$\Phi = 10^{-2}$		$\Phi = 10^{-1}$	
	n	α_n	C_n	α_n	C_n	α_n	C_n
	1	0.11774×10^{3}	-0.44909×10^{2}	0.35142×10^{2}	-0.14848×10^{2}	0.10634×10^{2}	-0.48592×10
	2	-0.63289×10	0.87702	-0.62966×10	0.92546	-0.58951×10	0.14948×10
	3	-0.39893×10^{2}	0.43528×10	-0.30007×10^{2}	0.11382×10^{2}	-0.11586×10^{2}	0.33503×10
	4	-0.91568×10^{2}	0.22542×10^{2}	-0.48609×10^{2}	0.24563×10	-0.44876×10^{2}	0.13321×10^{-1}
	5	-0.13158×10^{3}	0.15539×10^{2}	-0.11468×10^{3}	0.72674×10^{-1}	-0.11388×10^{3}	0.63751×10^{-3}
$B = 10$	6	-0.22015×10^{3}	0.12885×10	-0.21559×10^{3}	0.86815×10^{-2}	-0.21524×10^{3}	0.83446×10^{-4}
	7	-0.35086×10^{3}	0.21595	-0.34867×10^{3}	0.18373×10^{-2}	-0.34847×10^{3}	0.18081×10^{-4}
	8	-0.51524×10^{3}	0.57542×10^{-1}	-0.51392×10^{3}	0.53230×10^{-3}	-0.51379×10^{3}	0.52819×10^{-5}
	9	-0.71209×10^{3}	0.19763×10^{-1}	-0.71121×10^{3}	0.18943×10^{-3}	-0.71112×10^{3}	0.18863×10^{-5}
	10	-0.94114×10^{3}	0.80009×10^{-2}	-0.94051×10^{3}	0.78018×10^{-4}	-0.94045×10^{3}	0.77822×10^{-6}
	11	-0.12023×10^{4}	0.36431×10^{-2}	-0.12018×10^{4}	0.35853×10^{-4}	-0.12018×10^{4}	0.35796×10^{-6}
	12	-0.14955×10^{4}	0.18137×10^{-2}	-0.14952×10^{4}	0.17944×10^{-4}	-0.14951×10^{4}	0.17925×10^{-6}
	1	0.63371×10^{2}	-0.93263×10	0.16239×10^{2}	-0.36506×10	0.41462×10	-0.14176×10
	2	-0.26801×10	0.17703×10	-0.25725×10	0.17011×10	-0.19307×10	0.12312×10
	3	-0.27014×10^{2}	0.37393×10	-0.16417×10^{2}	0.18303×10	-0.90750×10	0.18517
	4	-0.64075×10^{2}	0.31147×10	-0.47091×10^{2}	0.11187	-0.44864×10^{2}	0.12167×10^{-2}
	5	-0.12244×10^{3}	0.58865	-0.11462×10^{3}	0.63126×10^{-2}	-0.11388×10^{3}	0.62869×10^{-4}
$B = 1$	6	-0.21920×10^{3}	0.86029×10^{-1}	-0.21559×10^{3}	0.83484×10^{-3}	-0.21524×10^{3}	0.83123×10^{-5}
	7	-0.35068×10^{3}	0.18539×10^{-1}	-0.34866×10^{3}	0.18102×10^{-3}	-0.34847×10^{3}	0.18054×10^{-5}
	8	-0.51519×10^{3}	0.53687×10^{-2}	-0.51392×10^{3}	0.52867×10^{-4}	-0.51379×10^{3}	0.52783×10^{-6}
	9	-0.71207×10^{3}	0.19065×10^{-2}	-0.71121×10^{3}	0.18875×10^{-4}	-0.71112×10^{3}	0.18856×10^{-6}
	10	-0.94114×10^{3}	0.78387×10^{-3}	-0.94051×10^{3}	0.77859×10^{-5}	-0.94045×10^{3}	0.77806×10^{-7}
	11	-0.12023×10^{4}	0.35978×10^{-3}	-0.12018×10^{4}	0.35809×10^{-5}	-0.12018×10^{4}	0.35792×10^{-7}
	12	-0.14955×10^{4}	0.17991×10^{-3}	-0.14952×10^{4}	0.17930×10^{-5}	-0.14951×10^{4}	0.17923×10^{-7}
	1	0.54079×10^{2}	-0.11574×10	0.12319×10^{2}	-0.54235	0.23971×10	-0.31159
	2	-0.38172	0.36429	-0.37706	0.35590	-0.33985	0.29505
	3	-0.23299×10^{2}	0.44764	-0.14796×10^{2}	0.17530	-0.89179×10	0.16415×10^{-1}
	4	-0.61401×10^{2}	0.28124	-0.46994×10^{2}	0.10415×10^{-1}	-0.44863×10^{2}	0.12060×10^{-3}
	5	-0.12194×10^{3}	0.53255×10^{-1}	-0.11462×10^{3}	0.62274×10^{-3}	-0.11388×10^{3}	0.62782×10^{-5}
$B = 0.1$	6	-0.21912×10^{3}	0.82918×10^{-2}	-0.21559×10^{3}	0.83161×10^{-4}	-0.21524×10^{3}	0.83090×10^{-6}
	7	-0.35066×10^{3}	0.18269×10^{-2}	-0.34866×10^{3}	0.18075×10^{-4}	-0.34847×10^{3}	0.18051×10^{-6}
	8	-0.51518×10^{3}	0.53322×10^{-3}	-0.51392×10^{3}	0.52831×10^{-5}	-0.51379×10^{3}	0.52779×10^{-7}
	9	-0.71207×10^{3}	0.18997×10^{-3}	-0.71121×10^{3}	0.18869×10^{-5}	-0.71112×10^{3}	0.18855×10^{-7}
	10	-0.94113×10^{3}	0.78227×10^{-4}	-0.94051×10^{3}	0.77844×10^{-6}	-0.94045×10^{3}	0.77805×10^{-8}
	11	-0.12023×10^{4}	0.35933×10^{-4}	-0.12018×10^{4}	0.35804×10^{-6}	-0.12018×10^{4}	0.35791×10^{-8}
	12	-0.14955×10^{4}	0.17976×10^{-4}	-0.14952×10^{4}	0.17928×10^{-6}	-0.14951×10^{4}	0.17923×10^{-8}

Table 2. Eigenvalues and coefficients for flat duct

		$\Phi = 10^{-3}$		$\Phi = 10^{-2}$		$\Phi = 10^{-1}$	
	n	α_n	C_n	α_n	C_n	α_n	C_n
$B = 10$	1	0.12827×10^{3}	-0.41806×10^{2}	0.37695×10^{2}	-0.13999×10^{2}	0.11271×10^{2}	-0.46264×10
	2	-0.19878×10	0.36861	-0.19865×10	0.37030	-0.19731×10	0.38739
	3	-0.20857×10^{2}	0.21588×10	-0.19814×10^{2}	0.35193×10	-0.10563×10^{2}	0.40904×10
	4	-0.58532×10^{2}	0.64331×10	-0.36928×10^{2}	0.94163×10	-0.24312×10^{2}	0.14367
	5	-0.10350×10^{3}	0.19951×10^{2}	-0.68490×10^{2}	0.62405	-0.66347×10^{2}	0.43056×10^{-2}
	6	-0.14593×10^{3}	0.10792×10^{2}	-0.13097×10^{3}	0.54748×10^{-1}	-0.13017×10^{3}	0.48926×10^{-3}
	7	-0.22137×10^{3}	0.15736×10	-0.21583×10^{3}	0.10274×10^{-1}	-0.21541×10^{3}	0.98274×10^{-4}
	8	-0.32579×10^{3}	0.34289	-0.32286×10^{3}	0.27817×10^{-2}	-0.32260×10^{3}	0.27239×10^{-4}
	9	-0.45258×10^{3}	0.10704	-0.45073×10^{3}	0.95538×10^{-3}	-0.45055×10^{3}	0.94460×10^{-5}
	10	-0.60125×10^{3}	0.41071×10^{-1}	-0.59996×10^{3}	0.38400×10^{-3}	-0.59983×10^{3}	0.38143×10^{-5}
	11	-0.77149×10^{3}	0.18086×10^{-1}	-0.77054×10^{3}	0.17333×10^{-3}	-0.77045×10^{3}	0.17260×10^{-5}
	12	-0.96318×10^{3}	0.88015×10^{-2}	-0.96246×10^{3}	0.85559×10^{-4}	-0.96239×10^{3}	0.85317×10^{-6}
$B = 1$	1	0.80588×10^{2}	-0.72742×10	0.21006×10^{2}	-0.27701×10	0.54839×10	-0.10725×10
	2	-0.72340	0.51929	-0.72097	0.51720	-0.69800	0.49730
	3	-0.15199×10^{2}	0.16643×10	-0.12361×10^{2}	0.16030×10	-0.61658×10	0.56425
	4	-0.45728×10^{2}	0.25375×10	-0.29477×10^{2}	0.60195	-0.24202×10^{2}	0.10512×10^{-1}
	5	-0.83915×10^{2}	0.19113×10	-0.68030×10^{2}	0.41568×10^{-1}	-0.66343×10^{2}	0.41317×10^{-3}
	6	-0.13916×10^{3}	0.49029	-0.13092×10^{3}	0.49149×10^{-2}	-0.13017×10^{3}	0.48407×10^{-4}
	7	-0.22021×10^{3}	0.10538	-0.21583×10^{3}	0.98794×10^{-3}	-0.21541×10^{3}	0.97893×10^{-5}
	8	-0.32550×10^{3}	0.28656×10^{-1}	-0.32285×10^{3}	0.27338×10^{-3}	-0.32260×10^{3}	0.27192×10^{-5}
	9	-0.45249×10^{3}	0.97732×10^{-2}	-0.45072×10^{3}	0.94693×10^{-4}	-0.45055×10^{3}	0.94376×10^{-6}
	10	-0.60121×10^{3}	0.39033×10^{-2}	-0.59996×10^{3}	0.38208×10^{-4}	-0.59983×10^{3}	0.38124×10^{-6}
	11	-0.77147×10^{3}	0.17539×10^{-2}	-0.77054×10^{3}	0.17281×10^{-4}	-0.77045×10^{3}	0.17255×10^{-6}
	12	-0.96318×10^{3}	0.86307×10^{-3}	-0.96246×10^{3}	0.85393×10^{-5}	-0.96239×10^{3}	0.85301×10^{-7}
$B = 0.1$	1	0.73655×10^{2}	-0.81882	0.18286×10^{2}	-0.33272	0.43654×10	-0.14823
	2	-0.96405×10^{-1}	0.92920×10^{-1}	-0.96327×10^{-1}	0.92776×10^{-1}	-0.95564×10^{-1}	0.91373×10^{-1}
	3	-0.13473×10^{2}	0.21898	-0.10823×10^{2}	0.18110	-0.56595×10	0.55787×10^{-1}
	4	-0.43358×10^{2}	0.27137	-0.28962×10^{2}	0.54213×10^{-1}	-0.24192×10^{2}	0.10210×10^{-2}
	5	-0.82264×10^{2}	0.17555	-0.67994×10^{2}	0.40045×10^{-2}	-0.66343×10^{2}	0.41148×10^{-4}
	6	-0.13873×10^{3}	0.45292×10^{-1}	-0.13092×10^{3}	0.48636×10^{-3}	-0.13017×10^{3}	0.48356×10^{-5}
	7	-0.22012×10^{3}	0.10157×10^{-1}	-0.21582×10^{3}	0.98412×10^{-4}	-0.21541×10^{3}	0.97855×10^{-6}
	8	-0.32548×10^{3}	0.28168×10^{-2}	-0.32285×10^{3}	0.27291×10^{-4}	-0.32260×10^{3}	0.27188×10^{-6}
	9	-0.45248×10^{3}	0.96868×10^{-3}	-0.45072×10^{3}	0.94609×10^{-5}	-0.45055×10^{3}	0.94367×10^{-7}
	10	-0.60121×10^{3}	0.38838×10^{-3}	-0.59996×10^{3}	0.38189×10^{-5}	-0.59983×10^{3}	0.38122×10^{-7}
	11	-0.77147×10^{3}	0.17486×10^{-3}	-0.77054×10^{3}	0.17275×10^{-5}	-0.77045×10^{3}	0.17254×10^{-7}
	12	-0.96317×10^{3}	0.86139×10^{-4}	-0.96246×10^{3}	0.85376×10^{-6}	-0.96239×10^{3}	0.85299×10^{-8}

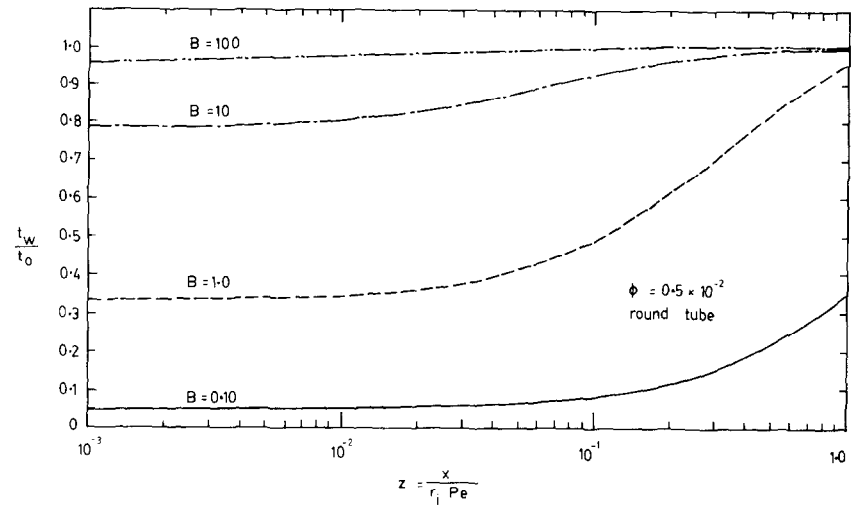

FIG. 4. Axial variation of wall temperature.

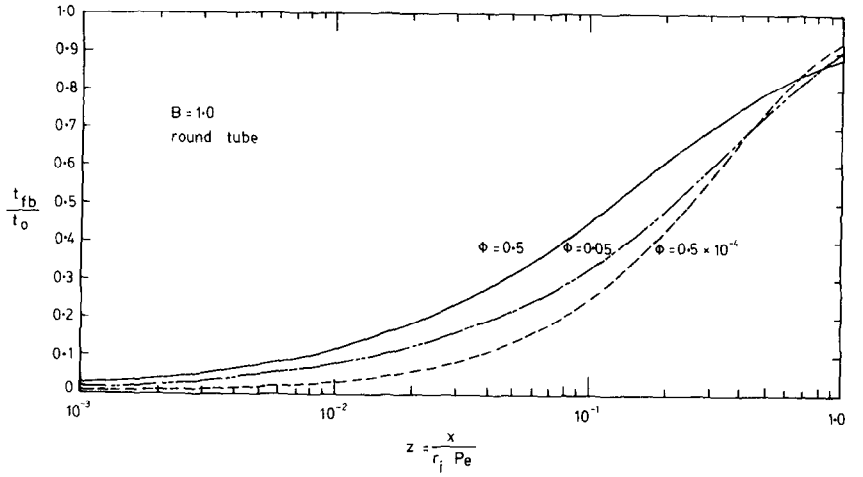

FIG. 5. Axial variation of bulk mean fluid temperature.

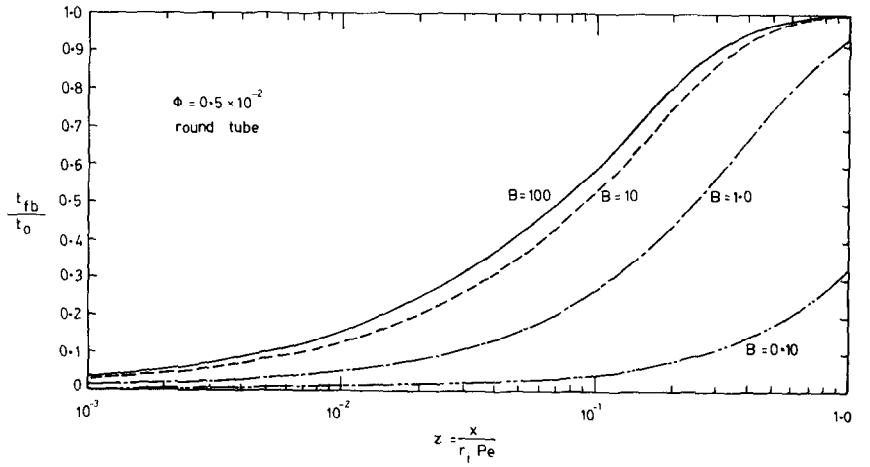

FIG. 6. Axial variation of bulk mean fluid temperature.

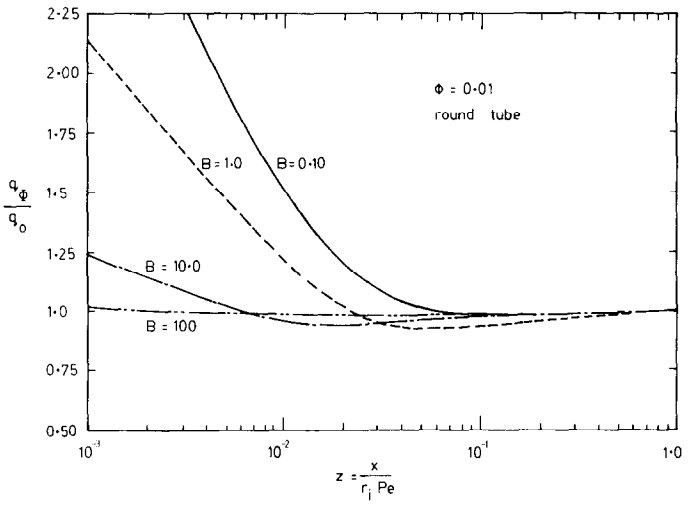

FIG. 7. Axial variation of wall heat flux.

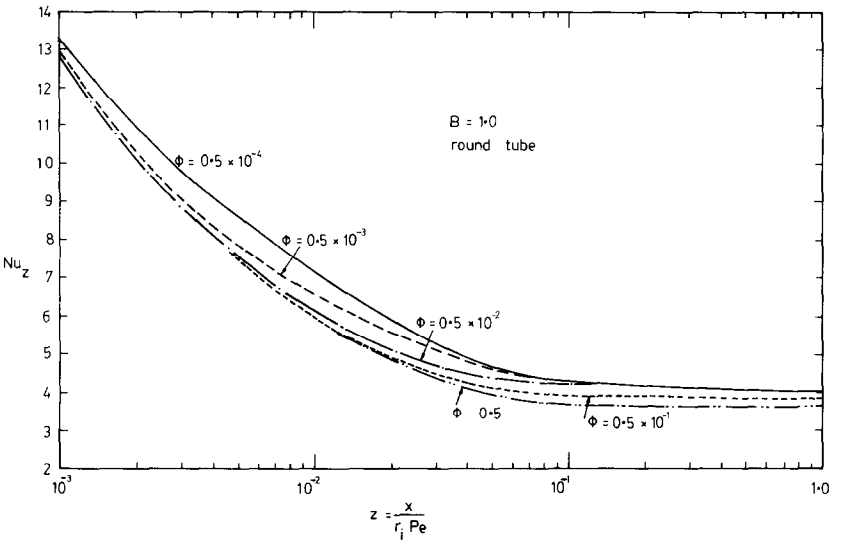

FIG. 8. Axial variation of local Nusselt number.

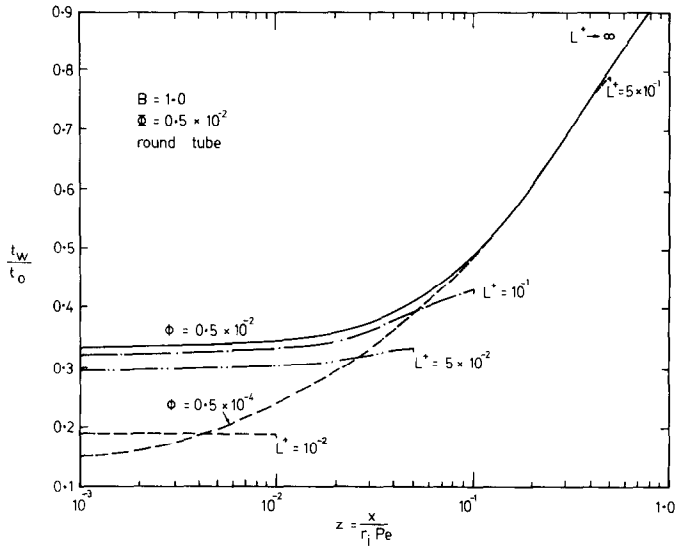

FIG. 9. Effect of total duct length on wall temperature.

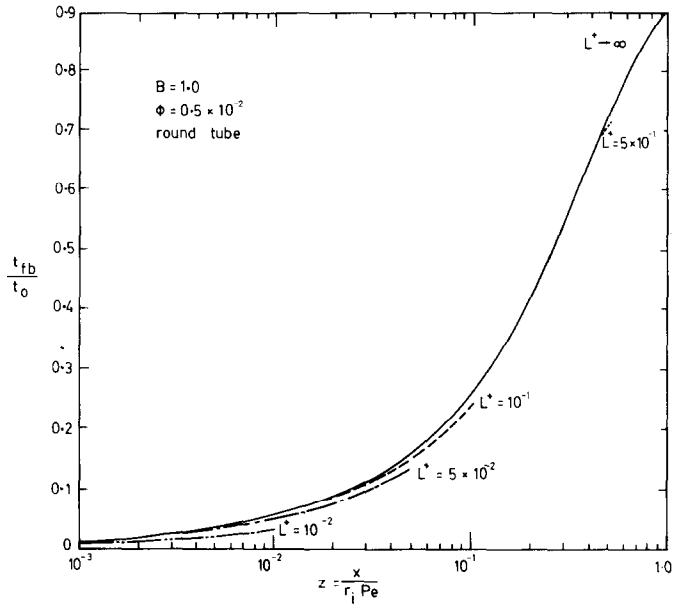

FIG. 10. Effect of total duct length on bulk mean fluid temperature.

8. An increase in the conduction parameter Φ reduces the local Nusselt number to different values along the tube. This again is due to the balance between, the heat flux, the wall temperature and the bulk mean fluid temperature, as these together determine the magnitude of the local Nusselt number.

The effect of the nondimensional duct length on the wall temperature and the bulk mean fluid temperature are shown in Figs. 9 and 10. When the length L^+ is more than about 0.2, the wall temperature follows closely the distribution for a 'long' duct. For shorter duct lengths, the wall temperature is significantly below that for the long duct. This is due to reduced heat flow from upstream due to the smaller length of the 'fin' available. The difference between the curves increases progressively as the duct length is reduced. When the conduction parameter is reduced to a small value ($\Phi = 0.5 \times 10^{-4}$), the difference between the wall temperature distribution for the long duct and a duct of length $L^+ = 1.0 \times 10^{-2}$ is very small and this difference is mainly near the end of the short duct. Similar trends of behaviour is observed at different Biot numbers, the effects of axial conduction being more pronounced at lower values of B.

The effect of the duct length on the bulk mean fluid temperature is less marked as seen in Fig. 10. The distribution for the shorter ducts follows the variation for the long duct closely.

The heat transfer results for the flat, rectangular duct follow the same trends as the circular tube. The

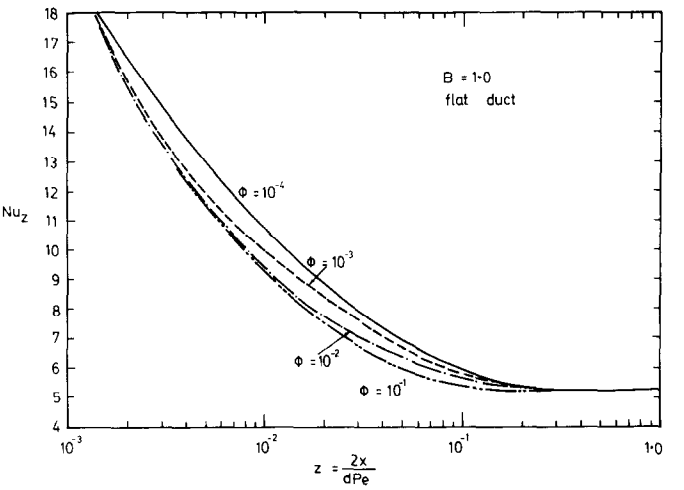

FIG. 11. Axial variation of local Nusselt number.

variation of local Nusselt number for this geometry is shown in Fig. 11, and the eigenvalues and coefficients for the problem are given in Table 2.

CONCLUSION

An analytical method based on the Laplace transform technique was obtained for the solution of conjugate heat transfer problem with axial wall conduction, external convection and internal laminar flow in round and flat ducts. The method is computationally simple and gives accurate results for the eigenvalues. It can be easily adopted for other flow situations.

The heat transfer parameters depend on four nondimensional groups B, Φ, z and L^+. For small values of the Biot number, B, the wall temperature distribution and the bulk mean fluid temperature distribution, depend strongly on the conductance parameter, Φ. The heat flux enhancement due to wall conduction is large at short distances from the duct inlet. The wall temperature is strongly dependent on the total duct length but the bulk mean fluid temperature is less dependent on the length. The variation of Nusselt number with Φ and B is significant.

REFERENCES

1. R. K. Shah and A. L. London, Laminar flow forced convection in ducts, Supplement 1 to *Advances in Heat Transfer*. Academic Press, New York, (1978).
2. R. K. Shah, Research needs in low Reynolds Number flow heat exchangers, *Heat Transfer Engng* **3**(2), 41–61 (1981).
3. E. J. Davis and W. N. Gill, The effect of axial conduction in the wall on heat transfer with laminar flow, *Int. J. Heat Mass Transfer* **13**, 459–470 (1970).
4. S. Mori, M. Sakakibara and A. Tanimoto, Steady heat transfer to laminar flow in a circular tube with conduction in the tube wall, *Heat Transfer–Jap. Res.* **3**(2), 37–46 (1974).
5. S. Mori, T. Shinke, M. Sakakibara and A. Tanimoto, Steady heat transfer to laminar flow between parallel plates with conduction in wall, *Heat Transfer–Jap. Res.* **5**(4), 17–25 (1978).
6. M. Faghri and E. M. Sparrow, Simultaneous wall and fluid axial conduction in laminar pipe-flow heat transfer, *Trans. Am. Soc. mech. Engrs*, Series C, *J. Heat Transfer* **102**, 58–62 (1980).
7. W. M. Kays, *Convective Heat and Mass Transfer*. McGraw-Hill, New York (1966).
8. M. Faghri and E. M. Sparrow, Forced convection in a horizontal pipe subjected to nonlinear external natural convection and to external radiation, *Int. J. Heat Mass Transfer* **23**, 861–872, (1980).
9. M. N. Özişik and M. S. Sadeghipour, Analytical solution for eigenvalues and coefficients of the Graetz problem with third kind boundary condition, *Int. J. Heat Mass Transfer* **25**, 736–739 (1980).

CONVECTION LAMINAIRE FORCEE DANS DES CONDUITS CIRCULAIRES ET PLATS AVEC UNE CONDUCTION AXIALE EN PAROI ET UNE CONVECTION EXTERNE

Résumé—Une solution analytique est obtenue pour la convection forcée laminaire dans des conduits circulaires et plats en présence de conduction axiale de paroi et de convection externe sur la surface externe de la paroi du conduit. Les valeurs propres du problème sont déterminées à partir d'une solution pour la condition aux limites de température uniforme. Le transfert thermique dépend de quatre nombres adimensionnels. Les températures de paroi et du fluide dépendent fortement du paramètre de conductance surfacique tandis que l'accroissement du flux de chaleur dû à la conduction de la paroi est important à des distances courtes de l'entrée du conduit.

KONVEKTION BEI ERZWUNGENER LAMINARER STRÖMUNG IN KREISFÖRMIGEN UND IN FLACHEN KANÄLEN MIT LÄNGSWÄRMELEITUNG IN DER WAND UND KONVEKTION AUF DER AUSSENSEITE

Zusammenfassung—Es wurde eine analytische Lösung für die Konvektion bei erzwungener laminarer Strömung in kreisförmigen und in flachen Kanälen bei Längswärmeleitung in der Wand und Konvektion an der Außenseite der Wand hergeleitet. Die Eigenwerte des Problems wurden unter Verwendung der Lösung für die Randbedingung konstanter Temperatur bestimmt. Die Ergebnisse für den Wärmedurchgang hängen von vier dimensionslosen Kennzahlen ab. Die Wand- und die Fluidtemperaturen hängen stark vom Wärmeleitfähigkeits-Parameter ab, während die Erhöhung der Wärmestromdichte infolge Längs-Wärmeleitung in der Wand bei geringen Abständen vom Kanaleintritt groß ist.

ЛАМИНАРНАЯ ВЫНУЖДЕННАЯ КОНВЕКЦИЯ В КРУГЛЫХ И ПЛОСКИХ КАНАЛАХ С ОСЕВОЙ ТЕПЛОПРОВОДНОСТЬЮ СТЕНОК И ВНЕШНЕЙ КОНВЕКЦИЕЙ

Аннотация—Получено аналитическое решение для ламинарной вынужденной конвекции в круглых и плоских каналах при осевой теплопроводности стенки канала и внешней конвекции на ее наружной поверхности. Собственные значения задачи найдены с помощью решения для граничных условий с постоянной температурой. Теплообмен определяется четырьмя безразмерными числами. Температуры стенки и жидкости сильно зависят от теплопроводности стенки, в то время как увеличение теплового потока из-за теплопроводности стенки заметно лишь на небольших расстояниях от входа в канал.